

An Empirical Method For Determination Of Kinetic Models And Kinetic Parameters Associated To Thermo-Oxidative Degradation Of Recycled Polypropylene (PP)

Helson M. da Costa^{*,**}, Valéria D. Ramos^{**}, Leonardo L. Esteves^{*}, Mônica C. de Andrade^{*}

^{*}Instituto Politécnico do Rio de Janeiro (IPRJ), Universidade do Estado do Rio de Janeiro (UERJ), Nova Friburgo, Rio de Janeiro (RJ), Brasil.

^{**} Universidade Estácio de Sá (UNESA), Nova Friburgo, Rio de Janeiro (RJ), Brasil.

Corresponding Author; Helson M. da Costa

ABSTRACT

The kinetics of thermo-oxidative degradation of polypropylene recycled (PP rec.) was investigated using thermogravimetric (TG) analysis in air atmosphere. An empirical methodology was developed, and it is the result of isoconversional methods (Kissinger-Akahira-Sunose and Ozawa-Flynn-Wall methods) combined with Coats-Redfern method, one-sample t test and IKP method. It was observed that the kinetic mechanism of the PP rec. degradation is dependent of the heating rate used. In lower heating rates, the diffusion mechanism is ruling, and D_i -type equations can be used. Otherwise, in higher heating rates the reaction rate is proportional to concentration of fraction remaining of reactant(s) raised to a power and F_i -type equations becomes as important as D_i -type equations. PP rec. sample was also submitted to eight extrusion cycles prior to TG analysis (PP rec. / 8), and it was noted that the mechanochemical degradation combined with thermo-oxidation produced an expressive reduction in the activation energy values. In addition, there was also a simplification of kinetic mechanism with only F_i -type equations being adequate for description of the process.

Keywords-Polypropylene, recycling, thermal analysis, degradation, kinetics

Date of Submission: 05-09-2018

Date of Acceptance: 21-09-2018

I. INTRODUCTION

One major problem associated with the applications of polymers is their instability to weathering. Organic materials are susceptible to attack by atmospheric oxygen and, in the case of synthetic organic polymers, oxidation degradation is often accelerated by environmental, biological and physical factors, e.g., sunlight, ozone, heat, radiation, mechanical stress, traces of transition metals ions, water, pollutants and micro-organisms [1-7].

In any of these situations, the oxidative processes lead to irreversible deterioration of the useful properties (e.g. mechanical properties: tensile, flexural and impact strengths; surface appearance: gloss, texture and color) of polymer artefacts and are reflected in poor performance or catastrophic failures. The extent of oxidative degradation, however, is not the same in all polymers: it depends on intrinsic chemical structure (the nature, number, and relative position of the chemical groups along the chain; magnitude of intramolecular forces – primary valence bonds – plus intermolecular forces – secondary valence bonds; crystallinity versus amorphicity; backbone rigidity; branch versus linear structures; crosslinking; etc.) and susceptibility to

external influences during lifetime of the polymer product. Among polymeric materials, polyolefins always receive considerable attention because possess high mechanical strength, low density, flexibility at low temperatures, high impact strength, good electrical insulation properties, etc. However, as in most other polymers, polyolefins are also susceptible to oxidative degradation and understanding about the mechanisms of the process has been the subject of intensive research over decades [3-7].

Once that thermal stability of polymer compounds is the most important factor for polymer applications, the extraction of the maximum relevant information from non-isothermal data, obtained by thermal analysis (TA) techniques, as well as the modelling of the kinetic process become critical tasks. Nevertheless, the problem of the validity and applicability of mathematical models in kinetic analysis of TA data is still considered a very controversial topic. Several authors have pointed out that the decomposition of a solid is a heterogeneous process and, therefore, the description of which with homogeneous equations is a meaningless exercise.

In addition, a single thermogravimetric analysis, for example, is considered unable to

distinguish between a mechanism governed by diffusion processes and those controlled by interface processes. Moreover, the kinetic parameters obtained are frequently dependent upon the experimental conditions, such as heating rate, atmosphere of the furnace, geometry of furnace, sample holder, speed of the recording device, particle size, and heat of reaction [1-7].

Despite a lot of research about degradation of polypropylene, in this manuscript, an empirical procedure for determination of kinetic parameters (pre-exponential factor, A; and, activation energy, E_a) and mechanisms associated with the degradation of recycled polypropylene, under thermo-oxidative conditions with air atmospheric, will be showed. Seeing that, in industry, knowledge of polymer behavior during extrusion on the production-plant scale is highly appreciated, we also adopted the same procedure for simulation and estimation of the stability of recycled polypropylene under mechanochemical degradation through of multiple extrusions.

1.1. Theoretical considerations

The thermal degradation of polymers has been studied quite extensively using thermogravimetric measurements. The mechanism of this process is very often unknown or too complicated to be characterized by a simple kinetic model. It tends to occur in multiple steps that have different rates. Anyway, processes in condensed phase are generally assumed as the product of two functions, one depending only on the temperature T and other depending only on the fraction transformed α (Equation 1) [8-10].

$$\frac{d\alpha}{dt} = k(T)f(\alpha) \quad \text{Eq. 1}$$

where α is the degree of conversion; T the temperature; $f(\alpha)$ is an algebraic expression usually associated with a physical model that describes the

kinetics of the solid-state reaction; and, $k(T)$ is a temperature dependent function given by the Arrhenius equation so that Eq.(1) takes to form of a kinetic triplet (Equation 2) [8-10]:

$$\frac{d\alpha}{dt} = A \cdot \exp\left(-\frac{E_a}{RT}\right) \cdot f(\alpha) \quad \text{Eq. 2}$$

with A being the pre-exponential factor; E_a the activation energy; and, R the gas constant. The reaction model $f(\alpha)$ may take various forms, which are summarized in Table 1.

To determine this triplet, several procedures have been proposed in the literature for the kinetics analysis of experimental data obtained under different temperature evolution conditions, i.e., isothermal, linear heating rate, modulated temperature, sample controlled. These methods can, in general, be categorized as: (i) isoconversional and (ii) model fitting methods. The isoconversional method is, in fact, a “model-free” method which assumes that the conversion function $f(\alpha)$ does not change with the variation of the heating rate for all values of α . It involves the measuring of the temperatures corresponding to fixed values of α by experiments at different heating rates β . The isoconversional methods are considered to give accurate values of the activation energy. The pre-exponential factor usually cannot be determined without the assumption of the reaction model $f(\alpha)$. On the other hand, model fitting methods of kinetic analysis depend on the reaction model and assume the Arrhenius temperature dependence of the rate constant $k(T)$. They do not achieve a clean separation between temperature dependent $k(T)$ and the reaction model $f(\alpha)$. Moreover, the temperature sensitivity of the reaction rate depends on the extent of conversion. As a result, these methods are approximate [8-10].

Table 1: Common expressions for solid-state reactions mechanisms, $f(\alpha)$ and $g(\alpha)$ [10-13]

N°	Mod.	$g(\alpha) = \int_0^{\alpha} d\alpha/f(\alpha)$	$f(\alpha)$	RATE DETERMINING MECHANISM
1. CHEMICAL PROCESS OR MECHANISM NON-INVOLVING EQUATIONS				
1	$F_{1/3}$	$1 - (1 - \alpha)^{2/3}$	$(3/2)(1 - \alpha)^{1/3}$	Chemical reaction
2	$F_{3/4}$	$1 - (1 - \alpha)^{1/4}$	$4(1 - \alpha)^{3/4}$	Chemical reaction
3	$F_{3/2}$	$(1 - \alpha)^{-1/2} - 1$	$2(1 - \alpha)^{3/2}$	Chemical reaction
4	F_2	$(1 - \alpha)^{-1} - 1$	$(1 - \alpha)^2$	Chemical reaction
5	F_3	$(1 - \alpha)^{-2} - 1$	$1/2 (1 - \alpha)^3$	Chemical reaction
6	F_4	$(1 - \alpha)^{-3} - 1$	$1/3 (1 - \alpha)^4$	Chemical reaction
7	G_1	$1 - (1 - \alpha)^2$	$1/[2(1 - \alpha)]$	Chemical reaction
8	G_2	$1 - (1 - \alpha)^3$	$1/[3(1 - \alpha)^2]$	Chemical reaction
9	G_3	$1 - (1 - \alpha)^4$	$1/[4(1 - \alpha)^3]$	Chemical reaction
2. ACCELERATORY RATE EQUATIONS				

10	$P_{3/2}$	$\alpha^{3/2}$	$(2/3)\alpha^{-1/2}$	Nucleation (power law)
11	$P_{1/2}$	$\alpha^{1/2}$	$2\alpha^{1/2}$	Nucleation (power law)
12	$P_{1/3}$	$\alpha^{1/3}$	$3\alpha^{2/3}$	Nucleation (power law)
13	$P_{1/4}$	$\alpha^{1/4}$	$4\alpha^{3/4}$	Nucleation (power law))
14	P_2	α^2	$(1/2)\alpha^{-1}$	Nucleation (parabolic law)
15	E_1	$\ln(\alpha)$	α	Nucleation (exponential law)
16	E_2	$\ln(\alpha^2)$	$\alpha/2$	Nucleation (exponential law)
3. SIGMOIDAL RATE EQUATIONS ORRANDOM NUCLEATION AND SUBSEQUENT GROWTH				
17	A_1	$-\ln(1-\alpha)$	$1-\alpha$	Random nucleation/first order (Mampel)
18	$A_{2/3}$	$[-\ln(1-\alpha)]^{3/2}$	$(2/3)(1-\alpha)[- \ln(1-\alpha)]^{-1/2}$	Random nucleation (Avrami-Erofeev)
19	$A_{3/2}$	$[-\ln(1-\alpha)]^{2/3}$	$(3/2)(1-\alpha)[- \ln(1-\alpha)]^{1/3}$	Random nucleation (Avrami-Erofeev)
20	$A_{3/4}$	$[-\ln(1-\alpha)]^{4/3}$	$(3/4)(1-\alpha)[- \ln(1-\alpha)]^{-1/3}$	Random nucleation (Avrami-Erofeev)
21	$A_{5/2}$	$[-\ln(1-\alpha)]^{2/5}$	$(5/2)(1-\alpha)[- \ln(1-\alpha)]^{3/5}$	Random nucleation (Avrami-Erofeev)
22	A_2	$[-\ln(1-\alpha)]^{1/2}$	$2(1-\alpha)[- \ln(1-\alpha)]^{1/2}$	Random nucleation (Avrami-Erofeev)
23	A_3	$[-\ln(1-\alpha)]^{1/3}$	$3(1-\alpha)[- \ln(1-\alpha)]^{2/3}$	Random nucleation (Avrami-Erofeev)
24	A_4	$[-\ln(1-\alpha)]^{1/4}$	$4(1-\alpha)[- \ln(1-\alpha)]^{3/4}$	Random nucleation (Avrami-Erofeev)
25	$A_{1/2}$	$[-\ln(1-\alpha)]^2$	$(1/2)(1-\alpha)[- \ln(1-\alpha)]^{-1}$	Random nucleation (Avrami-Erofeev)
26	$A_{1/3}$	$[-\ln(1-\alpha)]^3$	$(1/3)(1-\alpha)[- \ln(1-\alpha)]^{-2}$	Random nucleation (Avrami-Erofeev)
27	$A_{1/4}$	$[-\ln(1-\alpha)]^4$	$(1/4)(1-\alpha)[- \ln(1-\alpha)]^{-3}$	Random nucleation (Avrami-Erofeev)
28	B_1	$\ln[\alpha/(1-\alpha)]$	$\alpha/(1-\alpha)$	Branching nuclei (Prout-Tompkins)
4. DECELERATED RATE EQUATIONS (PHASE BOUNDARY REACTION)				
29	R_1	α	1	Contracting disk (one-dimensional movement of the phase boundary resulting from the nucleation. Zero order mechanism)
30	R_2	$1-(1-\alpha)^{1/2}$	$2(1-\alpha)^{1/2}$	Contracting cylinder (two-dimensional movement of the phase boundary. One-half order

31	R ₃	$1 - (1 - \alpha)^{1/3}$	$3(1 - \alpha)^{2/3}$	mechanism) Contracting sphere (three-dimensional movement of the phase boundary. Two-thirds order mechanism)
5. DECELERATORY RATE EQUATIONS(EQUATIONS BASED ON THE DIFFUSION MECHANISM)				
32	D ₁	α^2	$1/(2\alpha)$	One-dimensional diffusion (parabolic law)
33	D ₂	$\alpha + (1 - \alpha)\ln(1 - \alpha)$	$[-\ln(1 - \alpha)]^{-1}$	Two-dimensional diffusion (cylindrical symmetry)
34	D ₃	$[1 - (1 - \alpha)^{1/3}]^2$	$(3/2)(1 - \alpha)^{2/3}[1 - (1 - \alpha)^{1/3}]^{-1}$	Three-dimensional diffusion (spherical simmetry, Jander equation)
35	D ₄	$1 - (2/3)\alpha - (1 - \alpha)^{2/3}$	$(3/2)[(1 - \alpha)^{-1/3} - 1]^{-1}$	Three-dimensional diffusion (spherical symmetry, Ginstling- Brounshtein equation)
36	D ₅	$[(1 - \alpha)^{-1/3} - 1]^2$	$(3/2)(1 - \alpha)^{4/3}[(1 - \alpha)^{-1/3} - 1]^{-1}$	Three-dimensional diffusion (Crank equation)
37	D ₆	$[(1 + \alpha)^{1/3} - 1]^2$	$(3/2)(1 + \alpha)^{2/3}[(1 + \alpha)^{1/3} - 1]^{-1}$	Three-dimensional diffusion (Komatsu equation)
38	D ₇	$1 + (2/3)\alpha - (1 + \alpha)^{2/3}$	$(3/2)[(1 + \alpha)^{-1/3} - 1]^{-1}$	Three-dimensional diffusion
39	D ₈	$[(1 + \alpha)^{-1/3} - 1]^2$	$(3/2)(1 + \alpha)^{4/3}[(1 + \alpha)^{-1/3} - 1]^{-1}$	Three-dimensional diffusion (Zuravlev, Lesbhim e Temelman - ZLT equation)
6. OTHER KINETICAL EQUATIONS WITH UNJUSTIFIED MECHANISM				
40	G ₇	$[1 - (1 - \alpha)^{1/2}]^{1/2}$	$4\{(1 - \alpha)[1 - (1 - \alpha)^{1/2}]\}^{1/2}$	
41	G ₈	$[1 - (1 - \alpha)^{1/3}]^{1/2}$	$6\{(1 - \alpha)^{2/3}[1 - (1 - \alpha)^{1/3}]\}^{1/2}$	

In this manuscript, an empirical procedure was adopted for kinetic study of the degradation of the recycled polypropylene (thermo-oxidative and mechanochemical degradation). This method was based in the following steps:

Step 1: Determination of E_a values by isoconversional methods and one-sample t-test Two methods were selected for estimation of E_a values. Ozawa-Flynn-Wall (OFW) method involves the

measurement of the temperature T, corresponding to a fixed value of the degree of conversion α , from the experiments at different heating rates β . The OFW method is based on the Equation 3 [8-10].

$$\ln \beta = -1.056 \frac{E_a}{RT} + \text{Const.} \quad \text{Eq. 3}$$

The plot of $\ln \beta$ vs. $1/T$ gives the slope $-1.056E_a/R$ by which the activation energy has

been evaluated. If the determined activation energy is the same for the various values of α , the existence of a single-step reaction can be concluded with certainty. On the contrary, a change of E_a with increasing degree of conversion is a sign of a complex reaction mechanism that invalidates the separation of variables involved in the OFW analysis [8-10].

Kissinger-Akahira-Sunose (KAS) method was also selected. This method is based on the expression (Equation 4) [8-10]:

$$\ln\left(\frac{\beta}{T^2}\right) = \ln\left(\frac{AR}{E_a}\right) - \frac{E_a}{RT} \quad \text{Eq. 4}$$

The plot $\ln\left(\frac{\beta}{T^2}\right)$ vs. $1/T$ for constant conversion α allows one gets the activation energy (E_a) at a particular α value [8-10]. With E_a values found for each conversion α , one-sample t-test was applied using a confidence interval percentage of 95%. The assumptions for application of one-sample t-test were: (i) the data are continuous (not discrete); (ii) the data follow the normal probability distribution; (iii) The sample is a simple random sample from its population. This procedure was applied for to give the lower and upper limits of the confidence interval for the population mean based on the t distribution with $n - 1$ degrees of freedom. This confidence interval is more commonly used in practice because the true standard deviation is rarely known in practice.

Step 2: Model fitting and screening

We used one of the most popular model-fitting methods, Coats-Redfern (CR) method. This method is based on the Equation 5 [10-13]:

$$\ln\left(\frac{g_i(\alpha)}{T^2}\right) \cong \ln\left(\frac{A_i R}{\beta E_{a_i}}\right) - \frac{E_{a_i}}{RT} \quad \text{Eq. 5}$$

The graph of $\ln\left(\frac{g_i(\alpha)}{T^2}\right)$ vs. $1/T$ gives a straight line whose slope and intercept allow us to calculate E_a and A for a reaction model [8-10]. Each of the models $g_i(\alpha)$ presented in Table 1 was used and, from Eq.5, several E_a values were found. For screening of results, analysis of the correlation coefficients together with analysis of the confidence intervals for E_a were considered.

Step 3: The invariant kinetic parameter (IKP) method

Kinetic models, chosen in step 2, were used for application of IKP method. So, for constant β , a plot $\ln\left(\frac{g_i(\alpha)}{T^2}\right)$ vs. $1/T$ (see Eq.5) is straight line whose slope allows the evaluation of activation energy E_v and intercept, pre-exponential factor, A_v for each reaction model $g_i(\alpha)$. The same procedure was repeated to obtain the pairs (E_v , A_v) for different heating rates. In sequence, the calculation of

invariant activation parameters was done using the compensation relation (Equation 6) [10-13]:

$$\ln A_v = \alpha^* + \beta^* E_v \quad \text{Eq. 6}$$

Plotting $\ln A_v$ vs. E_v for different heating rates, the compensation effect parameters α^* and β^* were obtained. These parameters follow Equation 7 [10-13]:

$$\alpha^* = \ln A_{inv} - \beta^* E_{inv} \quad \text{Eq. 7}$$

Finally, the plot of α^* and β^* can provide the true values of E_{inv} and A_{inv} [10-13].

II. EXPERIMENTAL

Commercial recycled polypropylene (PP rec.), PPH.210.40.T, was purchased from Plastimil Inovações em Compostos e Recicladados, Vinhedo, São Paulo, Brasil. No purification was made in spite of possible presence of various stabilizers in the commercial pellets of the PP rec. According to specifications given in the data sheet, this thermoplastic is a homopolymer with high thermal stability, black color, and it is adequate to obtain automotive parts by extrusion. In Table 2, properties of PP rec. are listed.

Table 2: PP rec. properties

Parameter	Value
Melt flow index (ASTM D 1238; 230 °C; 2.16 kg)	12 g/10 min ⁻¹
Specific gravity (ASTM D 792)	1.2 g cm ⁻³
Filler content (FT-IT-18; 670 °C; 40 min)	40 %
Shrinkage (FT-IT-45)	0.7 %
Aging (forced ventilation oven, 150 °C)	> 700 h
Tensile strength (ASTM D 638)	25 MPa
Melting point (ASTM D 3418)	160 °C

For mechanochemical degradation, PP rec. was processed by extrusion with a single screw extruder, AX-35 model (diameter of 35 mm and L/D ratio of 22), AX Plásticos Máquinas Técnicas. The barrel zones temperatures were 180/190/200/210/220 °C. Strips of thickness of 3 mm were obtained and ground and, thus, some material was removed for characterization. This material was named as PP rec./8.

The thermo-oxidative degradation of PP rec. and PP rec./8 was performed a Simultaneous Thermal Analyzer, PerkinElmer, STA-6000 model, equipped with Pyris Thermal Analysis™ software, 10.1 version. Dynamic conditions adopted for thermogravimetry (TG) were: air atmosphere, 20 mL min⁻¹; sample mass adjusted for 10.0 ± 0.5 mg; temperature range from room temperature to 600 °C; open alumina pans; and, heating rates (β): 3 °C min⁻¹, 6 °C min⁻¹ and 12 °C min⁻¹. At each heating rate, the

measurement was repeated three times. Calibration procedure with respect to indium standard was employed.

III. RESULTS AND DISCUSSION

1.1. TG, DTG and DSC curves – preliminary analysis

In the Figures 1 and 2, TG, DTG and DSC curves are shown for PP rec. samples, and, in the Table 3, some parameters from these curves are also presented. The values of the initial temperature of decomposition (T_{onset}) are very important, since they could indicate which be the processing and manufacturing temperatures without continuing or initiating a process of decomposition. In air atmosphere, PP rec. begins to degrade at about 311 °C, considering 3 °C min⁻¹ as heating rate; whereas

PP rec. / 8, under same heating rate, shows T_{onset} at about 305 °C. The same behavior is found in other heating rates and this already proves that PP rec. has better heat resistance than PP rec. / 8. Like PP rec. / 8 sample was submitted to eight cycles of extrusion, the mechanochemical degradation was undoubtedly imposed together with the thermo-oxidative degradation. The shift of onset to higher temperature with increasing β is due to the shorter time required for a sample to reach a given temperature at the faster heating rates. This heating rate dependence is also indicated in the DTG curves, especially to PP rec. In all samples, it was also observed that a large amount residue was formed, between 32 wt% up to 35 wt%, because of filler present.

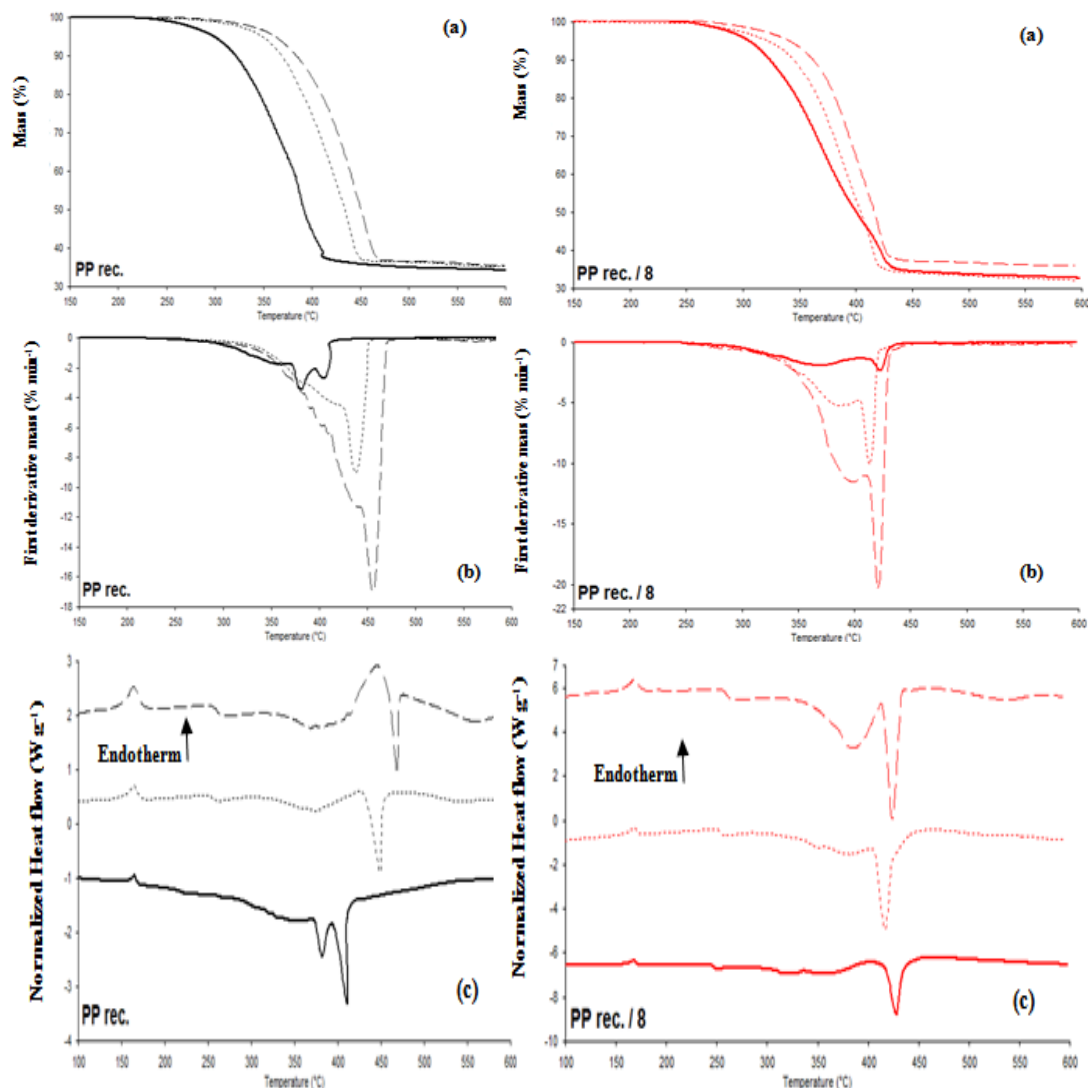


Figure 1: PP rec. curves. (a) termogravimetry (TG); (b) thermogravimetry derivative (DTG); and, (c)

differential scanning calorimetry (DSC). Heating rates: 3 °C min⁻¹ (solid line); 6 °C min⁻¹ (dotted line); and, 12 °C min⁻¹ (dashed line)

Figure 2: PP rec./8 curves. (a) termogravimetry (TG); (b) thermogravimetry derivative (DTG); and, (c) differential scanning calorimetry (DSC). Heating rates: 3 °C min⁻¹ (solid line); 6 °C min⁻¹ (dotted line); and, 12 °C min⁻¹ (dashed line)

Table 3: TG data for PP rec. samples

Sample	Parameters					
	T _{onset} (°C)	T _{endset} (°C)	T _M (°C)	t _{1/2} (min)	R* (%)	β**
PP rec.	311.4	417.2	405.3	124.1	32.2	3
	356.7	448.4	438.1	67.2	32.7	6
	386.2	467.3	455.6	34.4	35.9	12
PP rec. / 8	305.0	434.0	423.6	119.5	34.4	3
	338.7	422.9	414.0	63.2	35,3	6
	357.2	428.7	420.8	32.5	35.5	12

*R = Residue; ** : β = heating rate (°C min⁻¹)

Other representative parameters, from Figures 1 and 2 and Table 3, as T_M (peak of maximum temperature for the degradation process, which is estimated from DTG curve), T_{endset} (end of the degradation process), and t_{1/2} (half-time life) simply confirm the strong influence of the accentuated degradation imposed on the PP rec. / 8.

In addition, DTG curves reveal that the degradation of PP rec. or PP rec. / 8 cannot be represented through a single function for the mechanism of degradation, so a set of function must be used because of the different processes which occur during the degradation of the material. In fact, at least two degradation stages can be clearly identified in the DTG curves. Finally, DSC curves show that the melting temperature (T_m) of the thermoplastic is not altered, it is around 165 °C. At same time, DSC curves also exhibit the thermo-oxidative decomposition of the two PP rec. samples as oxidation reactions by means of exothermic peaks (temperature range from 350 ° up to 500 °C).

The behavior of the PP rec. / 8 sample can be explained by Yin et al. [14]. These authors describe that a mechanical recycling involves a series of treatments and preparation steps. Generally, the first stage of recycling process includes collecting, sorting, shredding, milling, washing, and drying the plastic waste into recycled plastic pellets, powder, or flakes.

In the second stage, the recycled plastic pellets, powder or flakes are molten and reprocessed into final products by resin molding technique. In agreement of this research, the current reprocessing techniques impose upon the recycled polyolefins irreversible changes in the polymeric structures -

molecular chain damages, including crosslinking, chain scission, and formation of double bonds.

Consequently, in keeping with these observations, PP rec. / 8 must be suffered considerable reduction of molar mass, long chains, and entanglements since high shear forces and high temperature, during multiple extrusions, severely degrade the recycled plastic.

In the Figure 3, the dependence of activation energy (E_a) on α for non-isothermal data, evaluated by different isoconversional procedures, for PP rec. samples is shown. In the PP rec. sample, E_a values found, by means of Kissinger-Akahira-Sunose (KAS) and Ozawa-Flynn-Wall (OFW) methods, were very similar. It is seen that the activation energy increases with degree of conversion, the activation energies obtained by isoconversional methods at lower conversion (0 % ≤ α ≤ 15%) were found to be significantly different from the activation energies obtained in the range 20% ≤ α ≤ 50%.

This should be ascribed to the nature of random scission degradation and the differences in deviation from stationary reaction state at different heating rates as suggested by Gao et al. [15]. The latter is a general characteristic of dynamic reaction. The former leads to production of a larger size of volatile fragments at higher temperature. The rate of weight loss at a definite temperature is therefore related not only to the scission rate of polymer chains, but also to the size of volatile products.

Despite this fact, normality test of Shapiro-Wilk was applied, and either KAS model or OFW passed with p-values of 0.134 and 0.115, respectively. KAS model showed t = 7.64 and, on 95% confidence interval, a mean global value for E_a should be found in the range of 118.0 up to 217.4 kJ mol⁻¹; whereas, OFW model exhibited t = 8.13 and, on 95% confidence interval, a mean global value for E_a should be observed in the range of 122.2 up to 216.3 kJ mol⁻¹.

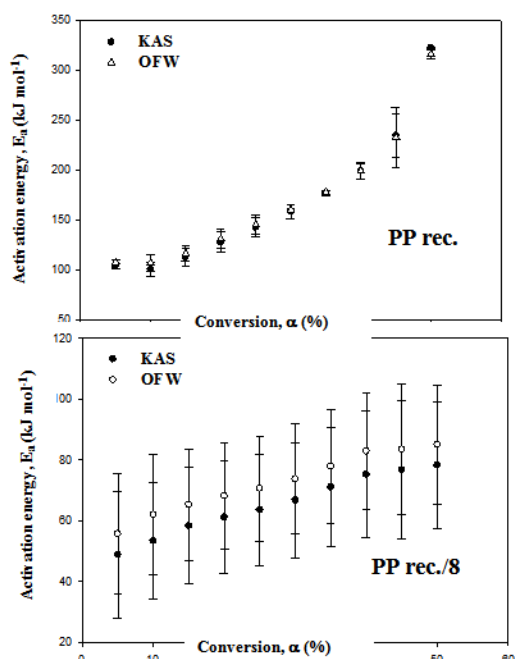


Figure 3: Dependence of activation energy (E_a) on α for non-isothermal data evaluated by different isoconversional procedures for PP rec. samples

Figure 3 also reveals that OFW and KAS models applied to PP rec. / 8 sample found difficulties to obey the linearity proposed by Equations 3 and 4, respectively. The values of E_a presented standard deviations greater than in the case of PP rec. sample. Notwithstanding this, same behavior was observed again – E_a increased together with increase of the conversion α . By all means, PP rec. / 8 also has not a unique degradation mechanism, though E_a values are lowest than that exhibited by PP rec.

As well as PP rec., PP rec. / 8 sample also exhibited validation of the normality hypothesis (Shapiro-Wilk test, KAS model with p-value of 0.710 and OFW model with p-value of 0.677). KAS model presented $t = 20.46$ and, on 95% confidence interval, mean global value for E_a should be found in the range of 58.0 up to 72.4 kJ mol^{-1} ; while, OFW model had $t = 23.07$ and, on 95% confidence interval, mean global value for E_a should be found in the range of 65.3 up to 79.4 kJ mol^{-1} .

1.2. Kinetic analysis and application of the empirical methodology

The degradation of polymers is a complex phenomenon, involving many simple reactions that are difficult to analyze separately. The quantitative contributions of these reactions to the degradation process are impossible to evaluate.

Bourbigot et al. [12] pointed that the degradation of a polymeric material often cannot be

represented by a single mechanism, so a set of function $f(\alpha)$ must be used because of the occurrence of many different elementary steps and complex mechanisms of thermal degradation. In the literature, as is well known, two types of kinetic models are generally applied for thermal degradation of polymers; one is the nth-order model with only parameter, i.e., reaction order; the other is a complex model containing several fitting parameters. In most cases, the nth-order model is adopted for its simplicity [16-18].

Succinctly, the autoxidation process of polymers involves free radical initiated chain reactions and proceeds in three basic steps: initiation, propagation and termination (Figure 4).

Many factors contribute to the initiation step leading to the formation of first alkyl macroradicals (Figure 4, reaction 1). Bimolecular oxygen-polymer reaction is generally not favored (very slow at moderate temperatures) on thermodynamic and kinetic grounds. Such a reaction take place only in polymers with very labile C – H bonds to give relatively stable alkyl radicals that terminate, rather than propagate, the oxidation chain reaction [4].

Propagation reactions involve the very fast reaction of oxygen diradical with polymer alkyl radicals leading to the formation of alkylperoxyl macroradicals (Figure 4, reaction 2). This is followed by abstraction of a hydrogen atom from another macromolecule resulting in hydroperoxide formation, the first molecular product of the chain oxidation process (Figure 4, reaction 3). This reaction involves the breaking of a C – H bond and, therefore, requires a higher activation energy than reaction 2.

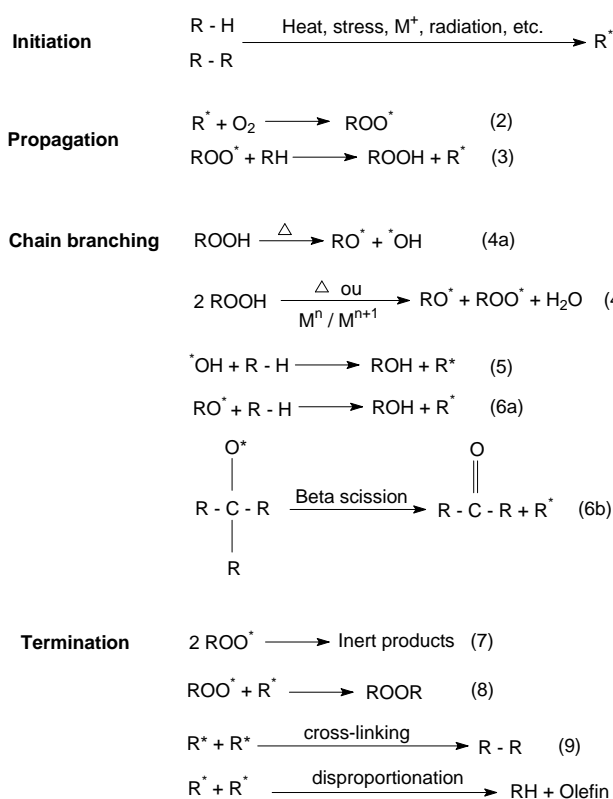


Figure 4: Basic autoxidation mechanism [4]

The rate of reaction 3, which in most polymers at normal oxygen pressures determines the overall oxidation rate, is a function of both the C – H bond dissociation energy (allyl < benzyl < tertiary < secondary < primary) and the stability of the alkyl macroradical formed. The hydroperoxide macromolecules formed can undergo homolysis under the effect of heat, light or metal ions giving rise to alkoxy and hydroxyl macroradicals (Figure 4, reaction 4). Both these radicals can abstract a hydrogen from another polymer molecule leading to new alkyl macroradicals (reactions 5 and 6a) which continue the chain reaction.

Alkoxy radicals can undergo further reactions, e.g. β -scission (reaction 6b), that would lead to cleavage of the macromolecular backbone and the generation of further radicals. Termination of the oxidative process occurs through combination or disproportionation reactions involving the various propagating radicals. The exact nature of the terminating step depends on both the structure of the polymer substrate and the oxygen concentration [4, 17-19].

The oxidation of polypropylene is highly heterogenous leading to regions where the polymer has a high concentration of peroxides and a mixture of other products. The heterogeneity of the overall oxidation is due to various chemical and physical factors such as structure and morphology of the

material, catalyst residues and other impurities as well as cage recombination of radicals and their different mobility and reactivity [17-19].

Polypropylene undergoes predominantly chain scission under all processing conditions giving rise to pronounced reduction in the molar mass and melt viscosity of the polymer. The propagation reaction (Figure 4, reaction 3) at the tertiary carbon atom of PP is 20 % more faster than a corresponding reaction at a secondary carbon atom (e.g. in PE). Furthermore, this reaction is particularly facilitated in PP by intramolecular hydrogen abstraction leading to the formation of adjacent hydroperoxides (less stable than isolated hydroperoxides) along the polymer chain resulting in an increased rate of initiation [4, 14-19].

In this way, there are numerous reactions involved in the degradation of PP and it is probable that the process is affected simultaneously by different mechanism or that when temperature increases, the decomposition mechanism changes.

For these reasons, we proposed an empirical methodology as described in 1.1. section. In the Figure 5, the correlations between $\ln A_v$ and E_v at different heating rates for PP rec. samples are exhibited; and, in Table 4, the compensation effect parameters α^* and β^* are shown.

Table 4: Compensation effect parameters, α^* and β^* , for PP rec. samples

Sample	Parameters			β ($^{\circ}\text{Cmin}^{-1}$)
	α^* (s^{-1})	β^* (mol kJ^{-1})	r^2	
PP rec.	-11.06	0.1965	0.853	3
	-2.91	0.1512	0.865	6
	-6.906	0.1693	0.854	12
PP rec. / 8	-10.27	0.2262	0.906	3
	-7.060	0.1774	0.993	6
	-7.206	0.1742	0.991	12

Coats-Redfern equation was employed for each $g(\alpha)$ model listed in Table 1 and, then, only $g(\alpha)$ functions that produced a better correlation (E_v in the range defined by one-sample t-test and $r^2 \rightarrow 1$) were chosen.

Models kinetics are generally classified based on the graphical shape of their isothermal curves (α vs t or $d\alpha/dt$ vs α) or on their mechanistic assumptions.

Based on their shape, kinetic models can be grouped into acceleratory, deceleratory, linear, or sigmoidal models. Acceleratory models are those in which the reaction rate ($d\alpha/dt$) is increasing (e.g., accelerating) as the reaction proceeds; similarly, deceleratory reaction rates decrease with reaction progress; while the rate remains constant for linear

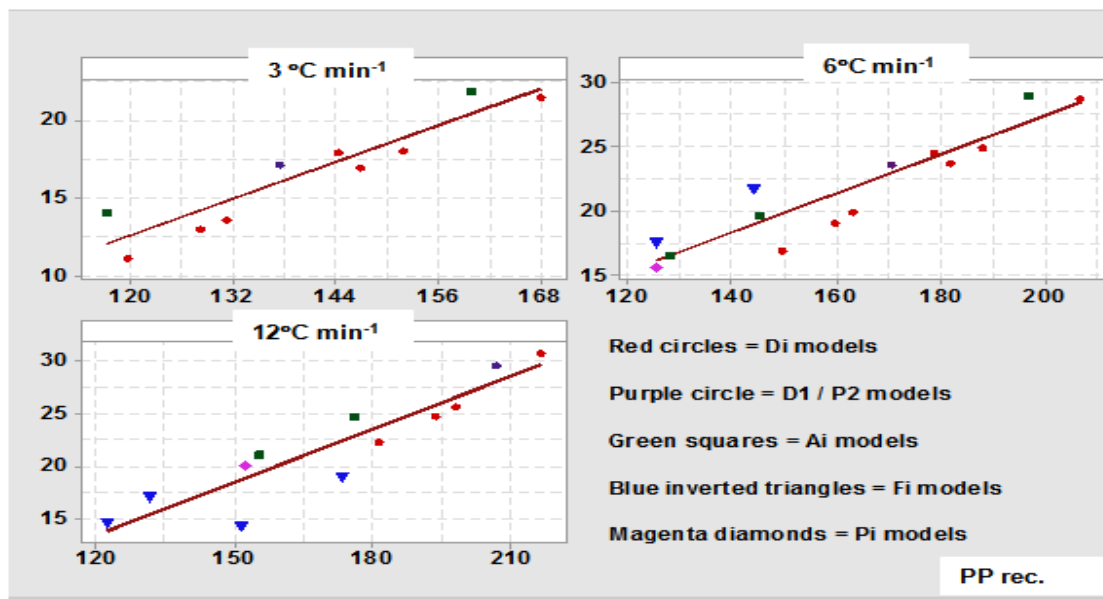
models; and, sigmoidal models show a bell-shaped relationship between rate and α [20].

From Figure 5, the influence of the heating rate on the evolution of the kinetic models for PP degradation is very clear.

For PP rec. sample, at $3\text{ }^{\circ}\text{C min}^{-1}$ there is a predominance of the diffusion mechanism defined by D_i -type equations, particularly three-dimensional diffusion. However, as heating rate increases to $6\text{ }^{\circ}\text{C min}^{-1}$ and $12\text{ }^{\circ}\text{C min}^{-1}$, D_i models are replaced, little by little, by other kinetic models and the kinetic mechanism defined by F_i -type equations (rate determining mechanism is chemical reaction) becomes as important as diffusion mechanism.

Khawam and Flanagan [20] point that one of the major differences between homogeneous and

heterogeneous kinetics is the mobility of constituents in the system. While reactant molecules are usually readily available to one another in homogeneous systems, solid-state reactions often occur between crystal lattices or with molecules that must permeate into lattices, where motion is restricted and may depend on lattice defects (diffusion-controlled reactions, D_i models). So, the rate of product formation decreases proportionally with the thickness of the product barrier layer. On the other hand, order-based (F_i) models are the simplest models, they are like those used in homogeneous kinetics. In these models, the reaction rate is proportional to concentration, amount or fraction remaining of reactant(s) raised to a power (integral or fractional) which is the reaction order.



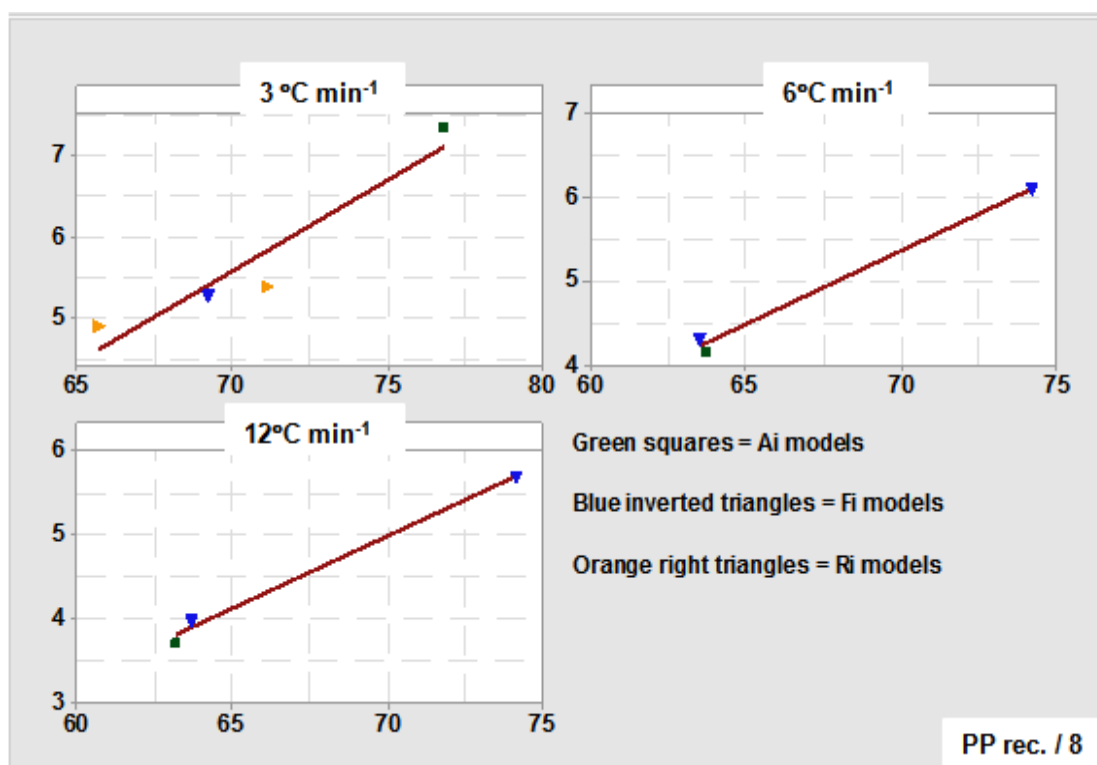


Figure 5: Correlation between $\ln A_v$ and E_a at different heating rates for PP rec. samples. The better kinetic models for correlation are shown

In this way, our hypothesis is that, in low heating rates as 3 °C min^{-1} , there is more time for the degradation process and, consequently, it is possible that the PP rec. degradation shows the initiation occurring through of large variety of mechanisms, as proposed by Achimsky et al. [19]. For instance: polymer thermolysis, monomer unit-oxygen interaction and participation of metallic impurities could be ways for the initiation. In addition, the propagation stage could present problems such as diffusion control of the reaction in thick samples, occurrence of a competitive intramolecular propagation and/or insolubility of oxygen in the crystalline phase, being attenuated. Another event, which it is probable in low heating rate, is the existence of mobility of the peroxy macro radicals that would favor a local propagation of oxidized domains from an “infectious” center or, in other words, an auto-accelerated character guaranteed for the oxidation kinetics. D_i models seem to respond better to these hypotheses and, thus, our experimental results would be corroborated.

Chan and Balke [21] studied the thermal degradation kinetics of polypropylene and defined two regions, separated by a relatively narrow transition region, for the mechanism. Region I, ranged from a conversion of approximately zero to about 10%, and a region II whose beginning varies according to heating rate.

In the region I there is little or no volatilization, the degree of scission is also low, and low value of E_a is generally attributed to the existence of weak points in the polymer. Commercial polypropylene contains a variety of oxidized functionalities (e.g $-\text{OOH}$, $=\text{OOR}$, $-\text{CO}-$, $-\text{CHO}$, $-\text{COOH}$, etc.) caused by processing and drying. These groups readily decompose to form free radicals. Also, polypropylene contains isotactic, atactic and syndiotactic triads that could have different energetics for degradation. There are also head-to-head and tail-to-tail enchainments in addition to the dominant head-to-tail placements, where the former can have different decomposition kinetics to the latter. Thus, the term “weak links” is a very broadly defined term.

On the other hand, region II is characterized by a large weight loss associated with high temperatures and high degree of chain scission. The average activation energy in this region is approximately the same of the carbo-carbon bond dissociation energy ($320 - 350\text{ kJ mol}^{-1}$) and it is associated with random scission throughout the polymer.

With increasing of the heating rate, β , time required for a sample to reach a given temperature is shortened. In keeping with this, the existence of multiple competing steps in polymer degradation will cause a change in the reaction mechanism; so that, the diffusion mechanism begins to replace for

others kinetic mechanisms faster and thermodynamically favored.

As mentioned by Khawam and Flanagan [20], F_i models are simpler and a pseudo first-order reaction must be predominant, as discussed by Chan and Balke [21], in higher heating rates (β values as $6\text{ }^\circ\text{C min}^{-1}$ and $12\text{ }^\circ\text{C min}^{-1}$) – it is shown in the Figure 5. These observations are in consonance with several researches present in the literature, which propose a random scission kinetic mechanism as “n-order” functions, and they could justify our experimental results.

For PP rec. / 8, it can be observed from Figure 5 that the degradation mechanism is simplest. Independently of β values, it seems like that only F_i models are need for to modeling of the reaction mechanism.

Hydrocarbon polymers are normally processed at high temperatures in the presence of mechanical shearing forces. Under these conditions, the polymer is subjected to a process of thermal degradation which is accelerated by atmospheric oxygen (ambient, dissolved or trapped in the polymer).

As consequence, various oxygen containing groups are introduced into the oxidized polymer substrate leading to changes in the molecular structure and the formation of low molecular mass products that would adversely affect the performance [2, 4-7].

PP rec. / 8 sample was submitted to eight extrusion cycles prior to the degradation thermo-oxidative by TG analysis; in front of this, during PP rec. melt extrusion process, oxygen dissolved in the polymer melt was consumed rapidly and, thus, in the environment inside closed extruder, oxygen concentration was diminished.

Thereby, the oxidation became oxygen diffusion limited and the concentration of R^* exceeded that of ROO^* in the polymer system (Figure 4, reactions 1 to 3). Rivatonet al. [5] pointed that the most widespread cause of heterogeneous degradation at the macroscopic levels results from oxygen diffusion-limited effects. These effects are likely to be observed under conditions of accelerated aging.

The importance of these effects depends on several parameters such as: sample thickness, oxygen consumption rate, sample temperature and others. If this all is true, D_i models can be neglected in favor of kinetic models such as F_i models, where reaction rate is proportional to concentration of fraction remaining of reactant(s) raised to a power, as it is suggested in the Figure 5.

The values of α^* and β^* parameters are presented in Table 4. In the Figure 6, plot of α^* versus β^* , which allows to obtain the true values of E_{inv} and A_{inv} , is shown.

Parameters α^* and β^* were obtained with reasonable regression coefficients (r^2 in the range of 0.86 up to 0.99), but A_{inv} and E_{inv} were determined with a good correlation ($r^2 \geq 0.98$).

Values found from Figure 6 seem to agree with all that was discussed in previous paragraphs – PP rec.: $E_{inv} = 177.8\text{ kJ mol}^{-1}$ and $\ln A_{inv} = 23.67$; PP rec. / 8: $E_{inv} = 61.92\text{ kJ mol}^{-1}$ and $\ln A_{inv} = 3.75$. Like PP rec. is a recycled material, these values, at first, may be reliable.

Figure 6: Evaluation of the pre-exponential factor and energy activation by means of IKP method for PP rec. samples

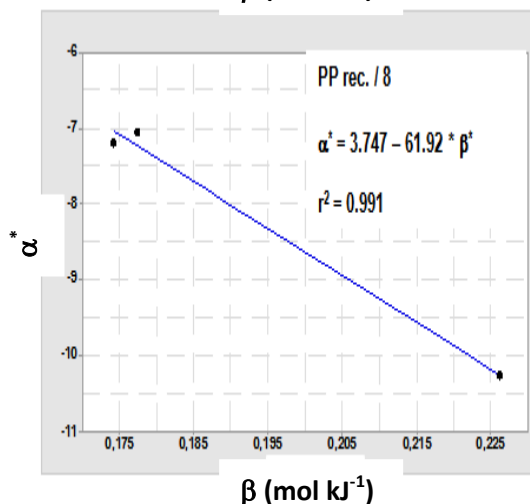
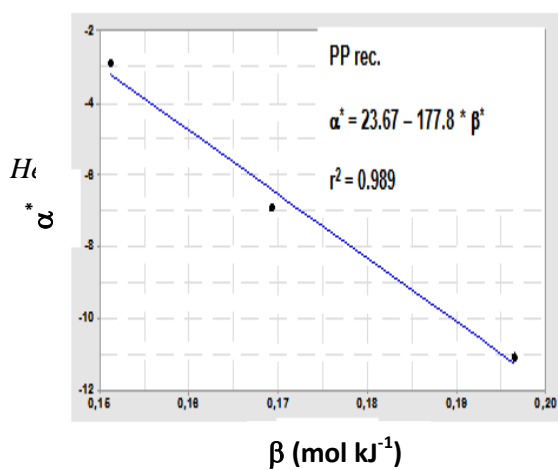
IV. CONCLUSIONS

An empirical methodology was proposed for the investigation of the PP degradation. Under the conditions experimental adopted, it was observed that the autoxidation process of PP rec. is dependent of the heating rate β .

For low values of β , such as $3\text{ }^\circ\text{C min}^{-1}$, a diffusion mechanism, modeled by D_i -type equations, is very important. With β value increasing, it was verified that, around $6\text{ }^\circ\text{C min}^{-1}$, F_i -type equations begin to be as important as D_i -type equations for interpretation of the degradation mechanism.

At $12\text{ }^\circ\text{C min}^{-1}$, F_i -type equations are present together with D_i -type equations in the same magnitude and, in this way, PP rec. degradation can be modeled as a chemical reaction of “n-order”.

Already in the PP rec. / 8 sample, it was seen that the mechanochemical degradation combined with the thermo-oxidative degradation not only produce low values of E_{inv} and A_{inv} , but also reduces the complexity of the kinetic mechanism to essentially F_i -type equations.



ACKNOWLEDGEMENTS

Authors thank the financial support of the CNPq, CAPES, FAPERJ and Programa Bolsa Pesquisa Produtividade UNESA/2018. Also, our thanks to the Laboratório de Biomateriais (IPRJ/UERJ).

REFERENCES

- [1]. B.R. Jadrnicek, S.S. Stivala, Kinetics of thermal oxidation of polyolefins – A review, *Polymer Engineering and Science*, 11(4), 1971, 265-273.
- [2]. S.S. Stivala, L. Reich, Structure vs stability in polymer degradation, *Polymer Engineering and Science*, 20(10), 1980, 654-661.
- [3]. G. Scott, Recent trends in the stabilization of polymers, *British Polymer Journal*, 15(4), 1983, 208-223.
- [4]. A. Al-Malaika, Oxidative degradation and stabilization of polymers, *International Materials Reviews*, 48(3), 2003, 165-185.
- [5]. A. Rivaton, J.L. Gardette, B. Mailhot, S. Marlat-Therlas, Basic aspects of polymer degradation, *Macromolecular Symposia*, 225(1), 2005, 129-146.
- [6]. X. Wang, X. Chen, W. Yu, Y. Ji, X. Hu, J. Xu, Applications of rheological torque-time curves to the study of thermooxidative degradation of polypropylene powder, *Journal of Applied Polymer Science*, 105(3), 2007, 1316-1330.
- [7]. J. Tochacek, J. Jancar, Processing degradation index (PDI) – A quantitative measure of

- processing stability of polypropylene, *Polymer Testing*, 31(8), 2012, 1115-1120.
- [8]. A. Pratap, T.L.S. Rao, K.N. Lad, H.D. Dhurandhar, Isoconversional vs. model fitting methods. A case study of crystallization kinetics of a Fe-based metallic glass, *Journal of Thermal Analysis and Calorimetry*, 89(2), 2007, 399-405.
- [9]. R. Ebrahimi-Kahrizsangi, M.H. Abbasi, Evaluation of reliability of Coats-Redfern method for kinetic analysis of non-isothermal TGA, *Transactions of Nonferrous Metals Society of China*, 18(1), 2008, 217-221.
- [10]. K. Chrissafis, Kinetics of thermal degradation of polymers. Complementary use of isoconversional and model-fitting methods, *Journal of Thermal Analysis and Calorimetry*, 95(1), 2009, 273-283.
- [11]. J.B. Dahiya, K. Kumar, M. Muller-Hagedorn, H. Bockhorn, Kinetics of isothermal and non-isothermal degradation of cellulose: model-based and model-free methods, *Polymer International*, 57(5), 2008, 722-729.
- [12]. S. Bourbigot, X. Flambard, S. Duquesne, Thermal degradation of poly(p-phenylenebenzobisoxazole) and poly(p-phenylenediamine terephthalamide) fibres, *Polymer International*, 50(1), 2001, 157-164.
- [13]. D. Trache, A. Abdelaziz, B. Siouani, A simple and linear isoconversional method to determine the pre-exponential factors and the mathematical reaction mechanism functions, *Journal of Thermal Analysis and Calorimetry*, 128(1), 2017, 335-348.
- [14]. S. Yin, R. Tuladhar, F. Shi, R.A. Shanks, M. Combe, T. Collister, Mechanical reprocessing of polyolefin waste: a review, *Polymer Engineering and Science*, 55(12), 2015, 2899-2909.
- [15]. Z. Gao, T. Kaneko, I. Amasaki, M.A. Nakada, A kinetic study of thermal degradation of polypropylene, *Polymer Degradation and Stability*, 80(2), 2003, 269-274.
- [16]. F. Doğan, Thermal decomposition behavior of oligo(4-hydroxyquinoline), *Polymer Engineering and Science*, 54(5), 2014, 992-1002.
- [17]. M. Celina, G.A. George, A heterogeneous model for the thermal oxidation of solid polypropylene from chemiluminescence analysis, *Polymer Degradation and Stability*, 40(3), 1993, 323-335.
- [18]. C. Albano, E. de Freitas, Thermogravimetric evaluation of the kinetics of decomposition of

- polyolefin blends, *Polymer Degradation and Stability*, 61(2), 1998, 289-295.
- [19]. L. Achimsky, L. Audouin, J. Verdu, Kinetic study of the thermal oxidation of polypropylene, *Polymer Degradation and Stability*, 57(3), 1997, 231-240.
- [20]. A. Khawam, D.R. Flanagan, Solid-state kinetic models: basics and mathematical fundamentals, *The Journal of Physical Chemistry B.*, 110(35), 2006, 17315-17328.
- [21]. J.H. Chan, S.T. Balke, The thermal degradation kinetics of polypropylene: Part III. Thermogravimetric analyses, *Polymer Degradation and Stability*, 57(2), 1997, 135-149.

Helson M. Da Costa "An Empirical Method For Determination Of Kinetic Models And Kinetic Parameters Associated To Thermo-Oxidative Degradation Of Recycled Polypropylene (PP)" *International Journal of Engineering Research and Applications (IJERA)*, vol. 8, no.9, 2018, pp 15-27